Journal of Cleaner Production 179 (2018) 217–224

Contents lists available at ScienceDirect

Journal of Cleaner Production

journal homepage: www.elsevier.com/locate/jclepro

Enhancement of bauxite residue as a low-cost adsorbent for phosphorus in aqueous solution, using seawater and gypsum treatments

Patricia B. Cusack [a, b, c], Mark G. Healy [b, *], Paraic C. Ryan [g], Ian T. Burke [d], Lisa M.T. O' Donoghue [e], Éva Ujaczki [c, e, f], Ronan Courtney [a, c]

[a] Department of Biological Sciences, University of Limerick, Castletroy, Co. Limerick, Ireland
[b] Civil Engineering, National University of Ireland, Galway, Ireland
[c] The Bernal Institute, University of Limerick, Castletroy, Co. Limerick, Ireland
[d] School of Earth and Environment, University of Leeds, Leeds, LS2 9JT, United Kingdom
[e] Design and Manufacturing Technology, University of Limerick, Castletroy, Co. Limerick, Ireland
[f] Department of Applied Biotechnology and Food Science, Faculty of Chemical Technology and Biotechnology, Budapest University of Technology and Economics, Müegyetem rkp. 3, 1111, Budapest, Hungary
[g] Discipline of Civil, Structural and Environmental Engineering, School of Engineering, University College Cork, Ireland

ARTICLE INFO

Article history:
Received 21 July 2017
Received in revised form
11 January 2018
Accepted 12 January 2018

Keywords:
Bauxite residue
Adsorption
Bauxite residue filter
Aqueous solution
Phosphate removal

ABSTRACT

Bauxite residue (red mud), the by-product produced in the alumina industry, is being produced at an estimated global rate of approximately 150 Mt per annum. Due to its highly alkaline nature, many refineries use neutralisation techniques such as mud farming (atmospheric carbonation), direct carbonation using carbon dioxide or reactions with seawater, to treat the bauxite residue and reduce its alkalinity prior to disposal in the BRDA (bauxite residue disposal area). Applying a treatment can render the bauxite residue non-hazardous and may also prepare the bauxite residue for reuse, particularly as an adsorbent. In this study, gypsum and seawater treatments were applied to the various bauxite residue samples obtained and the effects on its mineral, elemental and physiochemical properties were examined, as well as the effect on its phosphorus (P) adsorption capacity. It was found that in addition to reducing the alkalinity of all bauxite residue samples used, the P adsorption capacity was also enhanced following amendment with seawater or gypsum, particularly with gypsum. A positive correlation was detected between P adsorption and both Ca and CaO. A negative correlation was detected between the P adsorption and pH of the media. Fitting the data obtained from a batch adsorption experiment to the Langmuir adsorption isotherm, the maximum adsorption capacity was estimated to range from 0.345 to 2.73 mg P per g bauxite residue, highlighting the re-use potential for bauxite residue as an adsorbent for P.

1. Introduction

During the extraction of alumina from bauxite ore using the Bayer process, a by-product called bauxite residue (red mud) (Kirwan et al., 2013; Liu et al., 2014) is produced. The global inventory for bauxite residue is approximately 3 billion tonnes, with an estimated annual production rate of 150 million tonnes (Evans, 2016; Mayes et al., 2016). Bauxite residue is highly alkaline (pH > 10) (Goloran et al., 2013), with a high salinity and sodicity (Gräfe et al., 2009). Current best practice within this industry includes careful planning and management of highly engineered bauxite residue disposal areas (BRDAs), avoiding contamination of the surrounding environment (Prajapati et al., 2016). In addition, some refineries use neutralisation techniques for the bauxite residue before disposal into the BRDAs (Klauber et al., 2011; IAI, 2015; Evans, 2016). These techniques include (1) direct carbonation, whereby the residue slurry is treated with either carbon dioxide, sulfur dioxide gas, or undergoes intensive mud farming using amphirollers (atmospheric carbonation) (Cooling, 2007; Fois et al., 2007; Dilmore et al., 2009; Evans, 2016) (2) addition of spent acids

* Corresponding author.
E-mail address: mark.healy@nuigalway.ie (M.G. Healy).

https://doi.org/10.1016/j.jclepro.2018.01.092
0959-6526/

and/or gypsum ($CaSO_4.2H_2O$) (Kirwan et al., 2013), or (3) reaction of residues with seawater (Hanahan et al., 2004; Palmer and Frost, 2009; Couperthwaite et al., 2014).

Bauxite residues typically comprise very fine particles, ranging from 0.01 μm to 200 μm (Pradhan et al., 1996). Depending on the type of bauxite ore used, in some refineries the bauxite residue undergoes a separation technique during processing (Evans, 2016), which allows it to be separated into two main fractions: a fine fraction with a particle size <100 μm and a coarse fraction with a particle size >150 μm (Eastham et al., 2006; Jones et al., 2012). The coarse fraction mainly consists of quartz (SiO_2), whereas the fine fraction is dominated by iron (Fe) oxides (Snars and Gilkes, 2009). The ratio of the fine to coarse fraction produced is dependent on the bauxite ore used and the Bayer process employed (Li, 2001). Refineries which carry out the separation technique, have found use for the coarse fraction to create roadways to the BRDA and/or storage embankments (Evans, 2016). However, finding appropriate options for the re-use of the fine fraction bauxite residue remains elusive (Power et al., 2011; IAI, 2015).

Fine fraction bauxite residue comprises Fe oxides (20–45%) and aluminium (Al) oxides (10–22%) (IAI, 2015), which make it suitable as a medium to adsorb phosphorus (P). The European Commission (EC) has identified waste management as an important aspect of the "circular economy" (European Commission, 2015), so in recent years, emphasis has been placed on investigating alternative methods of P recovery from wastewater (Grace et al., 2015, 2016). A move from the more conventional methods of P recovery such as biological removal and chemical precipitation (Wang et al., 2008), to the use of low-cost adsorbents from industrial solid wastes, such as bauxite residue, have been examined. In comparison to standard P removal by sand, bauxite residue has a high P retention capacity (Vohla et al., 2007). However, its P removal potential is enhanced following treatment by heat, acid or gypsum (Table 1). Of the methods employed, acid and heat treatment have proved most successful in increasing the P adsorption capacity of the bauxite residue, with maximum adsorption capacities of up to 203 mg P g^{-1} bauxite being achieved (Liu et al., 2007) compared to untreated residue (0.20 mg P g^{-1}; Grace et al., 2015) (Table 1). However, whilst acid and heat treatments have proven to be very successful in increasing the adsorption capacity of bauxite residue, they are expensive, energy consuming (using high temperatures up to 700 °C) (Xue et al., 2016), and, without further treatment, do not allow for the easy reuse of the bauxite residue (e.g. as a possible media for plant growth) (Xue et al., 2016).

Treatments such as seawater or gypsum provide relatively inexpensive, alternative treatments, which may not only enhance the P adsorption capacity of the bauxite residue media, but may also help to improve its physicochemical characteristics. Seawater treatment improves bauxite's physical structure, due to the addition of magnesium (Mg) and calcium (Ca) which behave as flocculating agents, allowing many of the fine particles in bauxite residue to form more stable aggregates (Jones and Haynes, 2011), and a partial decrease in sodium (Na) due to ion exchange with Mg, Ca and potassium (K) (Hanahan et al., 2004). Seawater-treated bauxite residues also allow adsorbed P to become bio-available, unlike the metal cations which are unavailable, highlighting the P and metal retention capabilities (Fergusson, 2009). Revegetation of bauxite residue using gypsum has also improved plant growth by reducing its alkalinity and salinity, and improving the structure of the residue (Courtney et al., 2009; Courtney and Kirwan, 2012). In addition to this, modern alumina refineries are often located close to deep water ports, to allow for the bulk shipment of incoming bauxite (sometimes from multiple sources) to the refinery and/or for bulk shipment of alumina to aluminium smelters situated elsewhere. Therefore, there is ample scope for the increasing use of seawater neutralization technology for pre-treatment of residues in refineries not already employing treatments previously mentioned, prior to their deposition in the BRDA.

To the best of the authors' knowledge, no study has previously compared the use of raw seawater or gypsum treatments on the separate fractions of bauxite residue as a method of neutralisation and preparation for the re-use of bauxite residue in its separated and unseparated fractions as low-cost adsorbents and a potential source of P. The objectives of this study were to (1) characterise bauxite residue from two different sources, before and after treatment with seawater and gypsum, and to investigate their potential to release trace elements (2) investigate the effect of the treated bauxite residue on P adsorption (3) assess the impact of particle size, mineral and elemental (particularly Ca and Mg) composition of the bauxite residue on the adsorption of P.

2. Materials and methods

2.1. Sample preparation

A 1 kg sample of fresh bauxite residue was obtained from Alteo Gardanne [Gardanne, France (4327′9″N, 527′41″ E)], who operate a co-disposal method for fine and coarse fractions of bauxite. This sample will be referred to hereafter as UFR. One kilogram of mud-farmed bauxite residue samples (treated by atmospheric

Table 1
Phosphorus (P) adsorption studies that have been carried out using bauxite residues, untreated and treated residues, and their recovery efficiencies.

	P recovery technique	Factors investigated	Type of water	Initial P concentration of the water	P recovered	Reference
Untreated bauxite residue	Batch adsorption experiment	Kinetics, pH and temperature	Synthetic water	5-100 mg P L^{-1}	0.20 mg P g^{-1}	Grace et al., 2015
Gypsum Treated	Batch adsorption experiment	Contact time (3, 6, 24, 48hr)	Synthetic water	20-400 mg P L^{-1}	7.03 mg P g^{-1}	Lopez et al., 1998
Brine treated bauxite residue (Bauxsol™*)	Batch adsorption experiment	pH, ionic strength, time	Synthetic water	0.5–2 mg P L^{-1}	6.5–14.9 mg P g^{-1}	Akhurst et al., 2006
Acid and brine treated bauxite residue (Bauxsol™ [a])	Batch adsorption experiment	Kinetics and isotherms	Synthetic water	200 mg P L^{-1}	55.72 mg P g^{-1}	Ye et al., 2014
Heat treated bauxite residue	Batch adsorption experiment	Time, pH and initial concentration	Synthetic water	155 mg P L^{-1}	155.2 mg P g^{-1}	Liu et al., 2007
Acid and heat treated bauxite residue	Batch adsorption experiment	Time, pH and initial concentration	Synthetic water	155 mg P L^{-1}	202.9 mg P g^{-1}	Liu et al., 2007
Acid treated bauxite residue	Batch adsorption experiment	Acid type, pH	Synthetic water	1 mg P L^{-1}	1.1 mg P g^{-1}	Huang et al., 2008

[a] Bauxsol™ = neutralised bauxite residue produced using the Basecon™ procedure, which uses brines high in Ca^{2+} and Mg^{2+} (McConchie et al., 2001).

carbonation and therefore non-hazardous), were also obtained from Rusal Aughinish Alumina [Limerick, Ireland (5237′06″N, 904′19″W)], who separate the fine (particle sizes <100 μm) and coarse (particle sizes >150 μm) fraction of bauxite residue before disposal (IAI, 2015) in a ratio of 9:1 (fine: coarse). The fine and coarse fractions will be referred to hereafter as UF (untreated fine) and UC (untreated coarse).

Before any analysis or experiments were conducted, all bauxite residue samples were dried at 105 °C for 24 h. Once dry, the samples were pulverised using a mortar and pestle and sieved to a particle size <2 mm. 0.3 kg of each sample were then treated with either seawater (S) or laboratory-grade gypsum (G) (Lennox, Ireland), so two treatments were applied to each source of bauxite residue. S or G, placed after the above abbreviations, indicates the treatment applied. Gypsum was applied to the 0.3 kg bauxite residue samples at a ratio of 8% (w/w) (Lopez et al., 1998) and leached for 72 h in accordance with standard methods (British Standard Institution, 2002). Seawater amendment involved mixing with 0.3 kg bauxite at a ratio of 5:1 (v/w) (after Johnston et al., 2010), for 1 h, followed by a 12 h settlement period overnight. The bauxite residue and seawater mixture was then filtered through a 0.45 μm membrane using a vacuum pump. The treated bauxite residue samples were then oven dried for 24 h, pulverised with a mortar and pestle, and sieved to <2 mm in size.

2.2. Characterisation study

Untreated and treated bauxite samples were characterised (n = 3) for their physical, chemical, elemental and mineralogical properties. Soil pH and electrical conductivity (EC) were measured in an aqueous extract, using 5 g of bauxite residue sample in a 1:5 ratio (solid: liquid) (Courtney and Harrington, 2010). The bulk density (ρ_b) was determined after Blake (1965) and the particle density (ρ_p) after Blake and Hartge (1986) using 10 g of bauxite residue samples. Total pore space (S_t) was calculated using the values obtained for the bulk and particle densities (Danielson and Sutherland, 1986). The effective particle size analysis (PSA) was determined on particle sizes <53 μm using optical laser diffraction on the Malvern Zetasizer 3000HS® (Malvern, United Kingdom) with online autotitrator and a Horiba LA-920, and reported at specific cumulative % (10, 50 and 90%). Mineralogical detection was carried out using X-ray diffraction (XRD) on 1 g samples using a Philips X'Pert PRO MPD® (California, USA), whilst surface morphology and elemental detection were carried out using scanning electron microscopy (SEM) and energy-dispersive X-ray spectroscopy (EDS) on a Hitachi SU-70 (Berkshire, UK), using approximately 1 g samples. Quantification of the elemental content was carried out on 1 g samples by Brookside Laboratories (OH, USA) after digestion (EPA, 1996) using Inductively Coupled Plasma Atomic Emission Spectroscopy (ICP-AES) and elemental composition quantified using X-ray fluorescence (XRF). Measurement of the point of zero charge (PZCpH) was after Vakros et al. (2002) using 1 g samples, and cation exchange capacity (CEC) was determined using the K saturation technique (Thomas, 1982), using 5 g samples. Brunauer-Emmett-Teller specific surface area (SSA) and pore volume analysis were conducted on 1 g samples, which were degassed at 120 °C for 3 h prior to analysis carried out by Glantreo Laboratories (Cork, Ireland).

2.3. Phosphorus adsorption batch study

The P adsorption capacity of nine bauxite samples (untreated and gypsum/seawater treated samples) were examined in a bench-scale experiment. To conduct a P adsorption isotherm test, ortho-phosphorus (PO_4^{3-}-P) solutions were made up to known concentrations using potassium dihydrogen phosphate (K_2HPO_4) in distilled water. One gram of each of the sieved media was placed into a series of 50 ml-capacity containers and was overlain with 25 ml of the solutions. Each sample was then shaken in a reciprocal shaker at 250 rpm for 24 h. At t = 24 h, the supernatant water from each sample container was filtered using 0.45 μm filters and analysed immediately using a nutrient analyser (Konelab 20, Thermo Clinical Labsystems, Finland). The data obtained from the P adsorption batch studies were modelled using the Langmuir adsorption isotherm (McBride, 2000), which assumes monolayer adsorption on adsorption sites and allows for the estimation of the maximum P adsorption capacity (q_{max}) of the media:

$$q_i = q_{max}\left(\frac{k_a C_e}{1 + k_a C_e}\right) \quad (1)$$

where q_i is the quantity of the contaminant adsorbed per gram of media (g g^{-1}), C_e is the equilibrium contaminant concentration in the water (g m^{-3}), k_a is a measure of the affinity of the contaminant for the media (m^3 g^{-1}), and q_{max} is the maximum amount of the contaminant that can be adsorbed onto the media (g g^{-1}).

2.3.1. Mobilization of metals

To determine whether the residue media released trace elements, 25 ml of water was mixed with 1 g of media for 24 h and the supernatant was analysed by ICP-MS. The elements selected for detection were Al, arsenic (As), barium (Ba), beryllium (Be), boron (B), cadmium (Cd), Ca, chromium (Cr), copper (Cu), Fe, gallium (Ga), K, lead (Pb), Mg, manganese (Mn), mercury (Hg), molybdenum (Mo), Na, nickel (Ni), P, selenium (Se), silicon (Si), titanium (Ti), vanadium (V), and zinc (Zn).

2.4. Statistical analysis

Linear regression analysis was utilised to examine the extent of correlation between the individual characteristic parameters of the bauxite residue samples and bauxite adsorption, using Minitab. A Pearson correlation coefficient and a correlation p-value were determined to quantify correlation. The p-value represents the probability that the correlation between the bauxite residue characteristic in question and the response variable (adsorption) is zero i.e. the probability that there is no relationship between the two.

3. Results and discussion

3.1. Characterisation of bauxite residue

3.1.1. Effect of treatments on elemental and mineralogical composition

The mineral and total elemental composition of the three untreated bauxite residues [UF (untreated fine fraction), UC (untreated coarse fraction), and UFR (untreated co-disposed)] are shown in Tables 2 and 3. Bauxite residues are typically high in Fe and Al oxides (Liu et al., 2007), which was found to be the case in this study. The mineralogical composition present for all untreated samples was dominated by Fe_2O_3, Al_2O_3, SiO_2 and CaO. A decrease in Al_2O_3 was noted following treatment with the gypsum and the seawater in all samples, with an increase in CaO content noted in samples treated with gypsum.

XRD analysis showed that the main crystalline phases present in UF were haematite (Fe_2O_3), goethite (FeO(OH)), perovskite ($CaTiO_3$), boehmite (AlO(OH)), rutile (TiO_2), gibbsite $Al(OH)_3$ and sodalite $Na_8(Al_6Si_6O_{24})Cl_2$ (Figure S1 in the Supplementary Material). Similarly, the main minerals in UFR were haematite (Fe_2O_3),

Table 2
Mineralogical composition of the bauxite residues, untreated and treated.

Parameter	Untreated Fine (UF)	Fine + gypsum (UFG)	Fine + seawater (UFS)	Untreated Coarse (UC)	Coarse + gypsum (UCG)	Coarse + seawater (UCS)	Untreated French (UFR)	French + gypsum (UFRG)	French + seawater (UFRS)
Fe_2O_3 (%)	43.9 ± 1.1	40.6 ± 0.6	41.8 ± 1.2	64.0 ± 5.1	61.4 ± 3.0	69.9 ± 3.8	43.9 ± 0.6	47.9 ± 0.5	53.3 ± 5.8
Al_2O_3 (%)	12.7 ± 0.6	11.3 ± 1.0	11.1 ± 2.5	19.4 ± 1.8	11.1 ± 0.6	7.4 ± 0.7	14.0 ± 1.0	11.2 ± 0.3	11.4 ± 2.2
CaO (%)	5.9 ± 0.2	8.2 ± 0.5	4.4 ± 0.3	1.1 ± 0.2	7.6 ± 0.4	1.2 ± 0.1	5.6 ± 0.1	7.7 ± 0.3	3.2 ± 0.5
MgO (%)	3.6 ± 1.3	3.5 ± 0.8	3.1 ± 1.0	4.7 ± 1.8	3.6 ± 0.8	2.6 ± 0.6	4.1 ± 0.6	3.8 ± 0.9	3.2 ± 1.6
SiO_2 (%)	8.6 ± 0.7	8.5 ± 0.9	8.6 ± 1.7	2.6 ± 0.3	1.3 ± 0.2	1.4 ± 0.2	9.4 ± 0.5	5.1 ± 0.4	4.3 ± 0.3
TiO_2 (%)	2.4 ± 0.3	2.1 ± 0.6	2.7 ± 0.1	0.9 ± 0.1	1.0 ± 0.1	2.1 ± 0.6	2.5 ± 0.02	2.3 ± 0.1	2.3 ± 0.5
P_2O_5 (%)	0.6 ± 0.04	0.4 ± 0.02	0.4 ± 0.1	0.3 ± 0.02	0.2 ± 0.02	0.2 ± 0.06	0.5 ± 0.01	0.5 ± 0.02	0.5 ± 0.01

Table 3
Elemental composition of the bauxite residues, untreated and treated.

Parameter	Untreated Fine (UF)	Fine + gypsum (UFG)	Fine + seawater (UFS)	Untreated Coarse (UC)	Coarse + gypsum (UCG)	Coarse + seawater (UCS)	Untreated French (UFR)	French + gypsum (UFRG)	French + seawater (UFRS)
B (mg kg^{-1})	470 ± 8.81	425 ± 29	448 ± 13	615 ± 13.3	622 ± 29	722 ± 32.1	566 ± 18.9	539 ± 25	483.8 ± 31
Al (mg kg^{-1})	72538 ± 1390	81095 ± 1219	80608 ± 3090	45854 ± 2769	48851 ± 2336	45917 ± 2080	67295 ± 3343	65389 ± 1326	64189 ± 595
As (mg kg^{-1})	21.9 ± 1.73	9.7 ± 0.4	<LOD[a]	<LOD[a]	<LOD[a]	<LOD[a]	8.1 ± 0.2	9.75 ± 0.6	6.51 ± 0.43
Ba (mg kg^{-1})	43.8 ± 1.19	29.4 ± 5	33.3 ± 0.7	13.9 ± 1.01	18.3 ± 3.4	12.7 ± 2.8	45.7 ± 1.5	41.4 ± 1.4	49.4 ± 3.8
Cd (mg kg^{-1})	8.033 ± 0.16	7.02 ± 0.3	7.33 ± 0.19	10.7 ± 0.18	10.8 ± 0.5	11.8 ± 0.59	9.31 ± 0.2	8.87 ± 0.3	8.21 ± 0.3
Cr (mg kg^{-1})	1698 ± 37.2	933 ± 44	1170 ± 12.9	880 ± 3.8	817 ± 13	803 ± 21.3	1184 ± 15.9	1090 ± 9	1159 ± 31.2
Fe (mg kg^{-1})	338571 ± 3057	289459 ± 1859	298282 ± 4937	434739 ± 9980	460078 ± 23043	471204 ± 25753	353392 ± 10003	328114 ± 4498	332251 ± 3435
Pb (mg kg^{-1})	34.88 ± 0.54	27.8 ± 2.8	36.9 ± 0.8	29.56 ± 3.03	24.6 ± 3	22.06 ± 2.47	34.5 ± 0.9	32.3 ± 0.8	37.4 ± 2.1
Mg (mg kg^{-1})	122.28 ± 4.96	163 ± 37	1047 ± 25.6	18.32 ± 4.78	8.5 ± 2.21	511.6 ± 25.4	109 ± 3.9	150 ± 9	2203.8 ± 134
Mn(mg kg^{-1})	163 ± 2.63	140 ± 6.1	167 ± 6.8	187 ± 15.5	223 ± 99	185 ± 31.1	134 ± 0.9	139 ± 1.9	142.9 ± 4.2
Ni (mg kg^{-1})	18.6 ± 0.89	<LOD[a]	2.25 ± 0.2	3.54 ± 0.27	3.15 ± 0.5	4.18 ± 0.22	1.1 ± 0.1	1.24 ± 0.2	1.23 ± 0.3
K (mg kg^{-1})	391 ± 13.68	454 ± 29	1108 ± 41	255 ± 38	195 ± 23	556.99 ± 67.38	399 ± 13	359 ± 11	1048 ± 63.2
Si (mg kg^{-1})	223.5 ± 46.1	256 ± 92	245.7 ± 35	213 ± 6.6	234 ± 34	194.46 ± 10.58	276 ± 20	285 ± 34	258.5 ± 11.7
Na (mg kg^{-1})	28347 ± 553	38180 ± 352	41864 ± 2012	8804 ± 666	5935 ± 114	11101.55 ± 1121.8	25514 ± 317	23703 ± 499	31974 ± 1087
Ti (mg kg^{-1})	1395 ± 196	1309 ± 100	1265 ± 22	<LOD[a]	<LOD[a]	<LOD[a]	1382 ± 38	1288 ± 120	1233 ± 46
V(mg kg^{-1})	1050 ± 21.6	781 ± 29	777± 8	786 ± 23.6	731 ± 20	731.04 ± 23	1036 ± 12	920 ± 7	983 ± 21
Zn (mg kg^{-1})	50.7 ± 0.71	40.6 ± 1.2	42.6 ± 1.3	86.7 ± 1.7	82 ± 5.4	84.68 ± 4.2	55.8 ± 0.5	55.6 ± 1.17	57.3 ± 0.9
Ga(mg kg^{-1})	78.9 ± 2.02	81.2 ± 0.53	73.9 ± 0.6	71.8 ± 1.03	69.3 ± 2.3	73.5 ± 1.6	86.8 ± 1.3	78.6 ± 2	78.8 ± 0.9
Ca(mg kg^{-1})	46657 ± 832	51641 ± 485	17159 ± 413	4152 ± 490	12771 ± 823	4089.42 ± 588.32	15084 ± 358	42703 ± 2383	14820 ± 926
P(mg kg^{-1})	955 ± 0.57	962 ± 99	1018 ± 15	1040 ± 23	1011 ± 59	1039.6 ± 23	1298 ± 26	1220 ± 10	1320 ± 53.8
Be(mg kg^{-1})	<LOD[a]	<LOD[a]	<LOD[a]	<LOD[a]	<LOD[a]	<LOD[a]	<LOD[a]	<LOD[a]	<LOD[a]
Cu (mg kg^{-1})	<LOD[a]	<LOD[a]	<LOD[a]	<LOD[a]	<LOD[a]	<LOD[a]	<LOD[a]	<LOD[a]	<LOD[a]
Hg (mg kg^{-1})	<LOD[a]	<LOD[a]	<LOD[a]	<LOD[a]	<LOD[a]	<LOD[a]	<LOD[a]	<LOD[a]	<LOD[a]
Mo(mg kg^{-1})	<LOD[a]	<LOD[a]	<LOD[a]	<LOD[a]	<LOD[a]	<LOD[a]	<LOD[a]	<LOD[a]	<LOD[a]
Se (mg kg^{-1})	<LOD[a]	<LOD[a]	<LOD[a]	<LOD[a]	<LOD[a]	<LOD[a]	<LOD[a]	<LOD[a]	<LOD[a]

[a] <LOD = below the limits of detection.

goethite (FeO(OH)), boehmite (AlO(OH)), rutile (TiO_2), gibbsite $Al(OH)_3$ and sodalite $Na_8(Al_6Si_6O_{24})Cl_2$ (Figure S2). Boehmite (AlO(OH)), rutile (TiO_2), gibbsite $Al(OH)_3$ haematite (Fe_2O_3) were the predominant minerals present in UC (Figure S3). Following treatment with seawater and gypsum, a change in mineral phase in UFG, UFS, UFRS and UFRG occurred (Figure S4, S5, S6, S7). After treatment with gypsum, a higher presence of the calcium carbonate, calcite ($CaCO_3$), was detected in UFRG and UCG (Figure S7 and S8), and post seawater treatment, small peaks representing brucite ($Mg(OH)_2$ were detected in UFS and UCS (S5 and S9).

These findings are similar to previous studies that examined various neutralization techniques for bauxite residue (Gräfe et al., 2009). When seawater is added to bauxite residue, a reaction occurs where the hydroxide, carbonate and aluminate ions are eliminated due to a reaction involving Mg^{2+} and Ca^{2+} (from the seawater) (Gräfe et al., 2009; Palmer and Frost, 2009). This results in the formation of alkaline solids such as the calcium carbonates, calcite and brucite, which cause a buffering effect, evidenced in a shift of pH to between 8 and 9 (Power et al., 2011). The addition of gypsum ($CaSO_4$) results in a drop in the pH (approximately 8.6) due to the precipitation of excess hydroxides ($OH-$), aluminium hydroxides ($Al(OH)_4^-$), carbonates (CO_3^{2-}) to form calcium hydroxide/lime (Ca(OH)), tri-calcium aluminate (TCA), hydrocalumite and calcium carbonate ($CaCO_3$), which behave as buffers and maintain pH (Gräfe et al., 2009). The addition of Ca also flocculates and helps with the formation of more stable aggregates (Jones and Haynes, 2011).

An analysis of water samples (Table S1) to examine mobilisation of metals showed that As, Al and Cr were present in the leachate from the UFR sample, but decreased following gypsum and seawater treatments. Arsenic, Fe and Al were mobilised from the UF sample, but these concentrations were reduced following treatment with gypsum and seawater. Aluminium was mobilised from the UC. The reduction in Fe and Al following treatment with either gypsum or seawater is in line with previous studies, which have shown that water soluble Fe and Al decrease following gypsum application (Courtney and Timpson, 2005). Overall, Al still remained above the maximum allowable concentration (MAC) of 0.2 mg L^{-1} (200 μg L^{-1}) (EPA, 2014) for Al for drinking water. Sodium was still at a high level following gypsum and seawater treatments, ranging from 139.3 ± 3.2 to 153 ± 24.8 mg L^{-1} and 241.3 ± 26 to 388.7 ± 18.6 mg L^{-1}, respectively. The MAC for Na in drinking water is 200 mg L^{-1} (EPA, 2014).

3.1.2. Effect of treatments on physicochemical properties

The untreated bauxite residues had high pH (10.8 ± 0.12 to 11.9 ± 0.06) and EC (704 ± 90.8 to 1184 ± 48.8 μS cm^{-1}) (Table 4). Following treatment with gypsum and seawater, pH decreased and

Table 4
Physical and chemical characterisation of the bauxite residues, untreated and treated.

Parameter	Untreated Fine (UF)	Fine + gypsum (UFG)	Fine + seawater (UFS)	Untreated Coarse (UC)	Coarse + gypsum (UCG)	Coarse + seawater (UCS)	Untreated French (UFR)	French + gypsum (UFRG)	French + seawater (UFRS)
pH	10.8 ± 0.12	8.7 ± 0.04	9.02 ± 0.07	11.4 ± 0.29	6.79 ± 0.08	7.95 ± 0.16	11.9 ± 0.06	9.17 ± 0.02	9.49 ± 0.01
EC (μS cm^{-1})	704 ± 90.8	1338 ± 3.5	3080 ± 17.3	856 ± 1.53	909 ± 2	916 ± 1.53	1184 ± 48.8	1219 ± 7.21	5323 ± 172
% Water	23.5 ± 0.65	28.9 ± 0.6	32.1 ± 1.72	0.39 ± 0.2	0.82 ± 0.18	3.13 ± 0.72	28 ± 0.54	35.3 ± 1.32	36.5 ± 0.16
d_{10} (μm)[a]	0.6 ± 0.09	1.37 ± 0.23	1.26 ± 0.06	1.27 ± 0.47	1.11 ± 0.23	1.66 ± 0.83	1.3 ± 0.04	1.49 ± 0.06	1.08 ± 0.74
d_{50} (μm)[b]	2.43 ± 0.29	3.56 ± 0.59	3.52 ± 0.11	5.13 ± 0.63	3.69 ± 0.49	3.68 ± 0.4	3.7 ± 0.12	4.11 ± 0.39	3.47 ± 0.98
d_{90} (μm)[c]	6.02 ± 0.86	7.12 ± 1.98	7.69 ± 1.97	12.04 ± 1.27	9.51 ± 0.25	7.0 ± 0.13	10.11 ± 2.37	9.81 ± 2.68	7.17 ± 3.25
Total Pore Space (%)[d]	50.03 ± 2.25	50.73 ± 9.04	50.03 ± 1.75	9.63 ± 6.46	10.82 ± 1.09	7.65 ± 5.26	61.77 ± 1.16	53.6 ± 1.95	53.87 ± 0.78
Bulk Density (g cm^{-3})[e]	1.5 ± 0.02	1.5 ± 0.01	1.49 ± 0.01	2.53 ± 0.01	2.48 ± 0.03	2.55 ± 0.01	1.31 ± 0.03	1.32 ± 0.03	1.31 ± 0.02
Particle Size Density (g cm^{-3})[f]	2.99 ± 0.1	3.11 ± 0.5	2.94 ± 0.12	2.81 ± 0.21	2.65 ± 0.4	2.7 ± 0.14	3.41 ± 0.07	2.85 ± 0.08	2.85 ± 0.07
PZCpH[g]	6.96 ± 1.21	3.43 ± 0.73	6.28 ± 0.98	6.89 ± 0.09	3.11 ± 0.12	6.39 ± 0.51	6.16 ± 0.21	6.32 ± 0.51	4.43 ± 0.09
CEC (K)(cmol kg^{-1})[h]	63.3 ± 2.56	64.1 ± 3.41	60.1 ± 2.96	N/A[k]	N/A[k]	N/A[k]	57.5 ± 2.13	56.4 ± 3.49	48.9 ± 13.7
Total Pore Volume (cm^{-3} g^{-1})[i]	0.03	0.03	0.03	0.02	0.02	0.03	0.03	0.04	0.03
BET SSA (m^2 g^{-1})[j]	11.73	12.77	13.82	12.58	13.19	15.37	15.24	17.57	17.57

[a] d_{10} (μm) = the size of particles at 10% of the total particle distribution, expressed in μm.
[b] d_{50} (μm) = the median; the size of particles at 50% of the total particle distribution, expressed in μm.
[c] d_{90} (μm) = the size of particles at 90% of the total particle distribution, expressed in μm.
[d] Total Pore Space = the total pore space which may be calculated from particle density and bulk density.
[e] Bulk density = the mass of soil per unit volume, expressed as g cm^{-3}.
[f] Particle size density = the density of the solid particles, excluding pore spaces between them, expressed as g cm^{-3}.
[g] PZCpH = the pH at which the point of zero charge is occurring.
[h] CEC = the cation exchange capacity, expressed as cmol kg^{-1}.
[i] BET SSA = specific surface area analysed using Brunauer-Emmett-Teller isotherm and expressed as m^2 g^{-1}.
[j] Total Pore Volume = measurement of total pore volume expressed as cm^{-3} g^{-1}.
[k] N/A = not available.

EC increased. Changes for pH after treatment with either seawater or gypsum are due to precipitation of calcium carbonates such calcite, brucite and aragonite, which behave as buffers and maintain a reduced pH (Menzies et al., 2004), while the increase in EC is attributed to the introduction of excess Na^+ and Ca^{2+} (Gräfe et al., 2009). The pH of bauxite residue is normally within the range of 11–13 (Newson et al., 2006), but varies due to the type of bauxite ore, Bayer process, and neutralisation techniques used in the refinery. Both seawater (Menzies et al., 2004; Johnston et al., 2010) and gypsum applications (Jones and Haynes, 2011; Courtney and Kirwan, 2012; Lehoux et al., 2013) are recognised methods of reducing the alkalinity of bauxite residues.

No change was observed in the particle size or particle size density following the addition of the gypsum and seawater treatments to the various bauxite residue samples (Table 4). Similarly, the addition of gypsum or seawater did not have any impact on bulk density (Table 4).

The surface morphology of bauxite residues typically comprises 30% amorphous and 70% crystalline phase (Gräfe et al., 2009). However, in this study SEM imaging suggests that the bauxite residue samples were not present in strong crystalline form (Fig. 1), in particular for samples UF and UFR, as no distinctive crystalline structure to the bauxite residue samples was observed. Liu et al. (2007) examined the effect of age on stored bauxite residue, and found that fresh bauxite residue particles are present in poorly formed crystallised or amorphous form in comparison to older bauxite residue (10 years), which has a stronger crystalline formation, indicating that crystallisation occurs in some of the minerals over time. As the bauxite residue used in this study was fresh, this would explain why there was not a strong distinction between amorphous or crystalline forms, similar to the findings of Liu et al. (2007). The composition of fine particles and larger particles in the coarse fraction (UC) were noticeable from the SEM (Fig. 1).

Improved aggregate formation was noticeable in the gypsum and seawater-treated bauxite residues (Fig. 1), due to the addition of Ca^{2+}, which results in flocculation (Zhu et al., 2016). Changes in the surface morphology were also evident in the gypsum and seawater-treated residues in comparison to the untreated residues, which appeared to have a much smoother surface (Fig. 1). This change in surface morphology following the treatments was attributed to the changes in mineral phase (Huang et al., 2008).

3.2. Phosphorus adsorption study

3.2.1. Effect of seawater and gypsum treatment on P adsorption

All nine bauxite residue samples in this study were successful in removing P from aqueous solution (Table 5). Bauxite residue has been shown in numerous P adsorption studies to have a high P retention capacity, particularly following treatment or modification (Ye et al., 2014; Grace et al., 2015). In this study, gypsum or seawater treatment had a positive impact on P removal, with the gypsum-treated bauxite residue performing best (Table 5).

Following seawater treatment, the P adsorption capacity of the bauxite residues increased to q_{max} values of 0.48, 0.66 and 1.92 mg P g^{-1} media for UFS, UCS and UFRS, respectively. In previous studies, following treatment with seawater, bauxite residue had a higher adsorption capacity for P. Akhurst et al. (2006) reported a maximum adsorption of 6.5 mg P g^{-1} when using a bauxite residue treated with brine (Bauxsol™). This relatively high adsorption may be attributed to the higher concentrations of Ca^{2+} and Mg^{2+} in the brines (or products such as Bauxsol™, developed by Basecon™), in comparison to raw seawater (0.41, 1.29 and 10.77 g kg^{-1} of Ca^{2+}, Na and Mg^{2+}, respectively) used in this study (Gräfe et al., 2009). The gypsum-treated bauxite residues had the highest q_{max} values – 2.46, 1.39 and 2.73 mg P g^{-1} media for UFG, UCG and UFRG, respectively. However, these values were lower than a P adsorption study carried out by Lopez et al. (1998), who used the same application rate of gypsum to the bauxite residue samples and reported a q_{max} of 7.03 mg P g^{-1}. The lower rate observed in the current study may be attributed to the 72 h leaching process that the gypsum-treated bauxite residue underwent before use in the adsorption study, which may have allowed

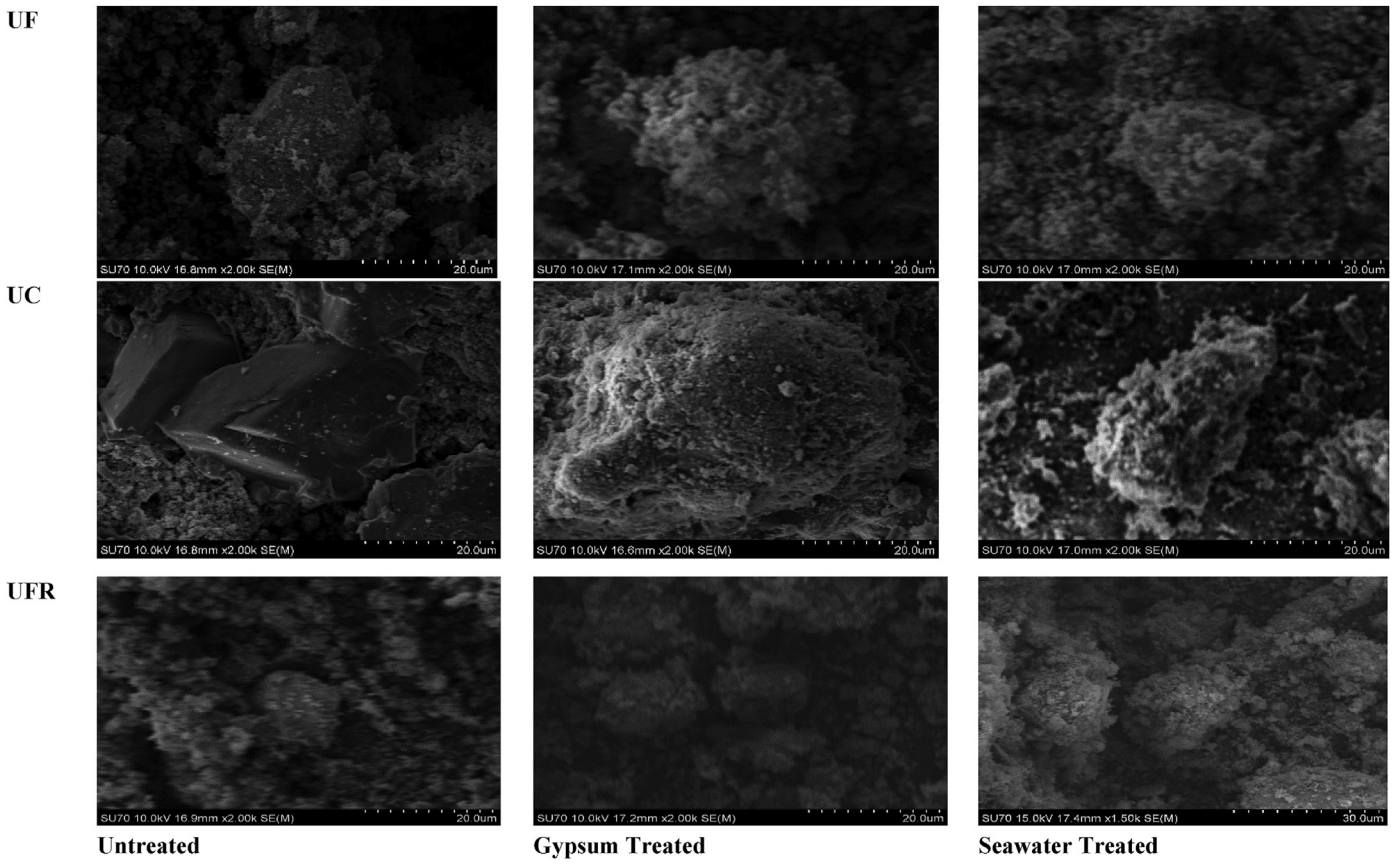

Fig. 1. SEM (10 kV; magnification ×2,000; working distance 16.8 mm) imaging for the three untreated bauxite residue pre and post treatment with either gypsum or seawater.

Table 5
Maximum adsorbency (mg P g^{-1} media) of P using each of the bauxite residue samples, untreated and treated (level of fit of the data, R^2, to Langmuir isotherm is included in brackets).

Media	Treatment method employed		
	Untreated	Gypsum	Seawater
	mg P g^{-1} media		
UFR	1 (0.99)	2.73 (0.99)	1.92 (0.99)
UF	0.38 (0.99)	2.46 (0.97)	0.48 (0.99)
UC	0.35(0.98)	1.39 (0.99)	0.66 (0.99)

for further exchange and removal of Ca^{2+} following the leaching process.

Overall, the bauxite residue in the current study had a higher P adsorbency than in other studies for zeolite (0.01 mg P g^{-1}, Grace et al., 2015) and granular ceramics (0.9 mg g^{-1}; Chen et al., 2012), but lower than fly ash, granular blast furnace slag and pyritic fill (6.48, 3.61 and 0.88 mg P g^{-1}, respectively; Grace et al., 2015), crushed concrete (19.6 mg P g^{-1}; Egemose et al., 2012), untreated biochar (32 mg P g^{-1}; Wang et al., 2015), and NaOH-modified coconut shell powder (200 mg P g^{-1}; de Lima et al., 2012).

3.2.2. Factors affecting P adsorption

The adsorption of P onto media is influenced by many factors which include particle size, pH, component and surface characteristics (Wang et al., 2016). Numerous studies have investigated the effect of parameters such as kinetics of P adsorption (Akhurst et al., 2006; Liu et al., 2007; Ye et al., 2014; Grace et al., 2015), ionic solution (Akhurst et al., 2006), pH (Liu et al., 2007; Huang et al., 2008; Grace et al., 2015) on the adsorption of P from aqueous solution. While all bauxite residue samples in this study did remove P from aqueous solution, it is clear that the application of treatments, such as gypsum or seawater, has an effect on the adsorption capability, and that the rate of adsorption will vary as a result of the source of bauxite residue and treatments used (Wang et al., 2008).

The parameters which showed a statistically significant positive correlation of medium strength with P adsorption in this study were Ca (correlation coefficient = 0.47, p = .01, Degrees of Freedom (DoF) = 25) and CaO (correlation coefficient = 0.39, p = .04, DoF = 25). A statistically significant negative correlation of medium strength was also detected between pH and P adsorption (correlation coefficient = - 0.38, p = .05, DoF = 25). pH was a contributing factor to the adsorption process with the amount of phosphate adsorbed increasing with a decrease in pH in the media following treatments, UFRG > UFRS > UFR, UFG > UFS > UF, UCG > UCS > UC. This was a similar finding to several studies carried out (Li et al., 2006; Liu et al., 2007; Huang et al., 2008; Grace et al., 2015). The Ca ions also influenced P adsorption. This is as a result of the high level of Ca^{2+} and Mg^{2+} present in the bauxite residue, particularly after seawater and gypsum treatments, when the majority of PO_4^{3-} is removed from solution due to the formation of magnesium phosphate ($Mg_3(PO_4)_2$) and calcium phosphate ($Ca_3(PO_4)_2$) (Akhurst et al., 2006).

The pH at which net charges are neutral on the surface of the adsorbent - the point of zero charge (PZC) - influences the rate of adsorption of P (Jacukowicz-Sobala et al., 2015). Where the pH is higher than the PZCpH, the surface of the adsorbent media becomes more negative (attracting more cations), as a result of the adsorption of OH^- from the surrounding solution (Prajapati et al.,

2016). The PZCpH ranged from 6.16 ± 0.21 to 6.96 ± 1.21 (Table 4) in the three untreated samples. Following treatment with gypsum and seawater, there were notable changes, but no statistical relevance was detected between the PZCpH and P adsorption in this study. However, as bauxite residue is composed of numerous minerals, each with their own individual PZCpH (which, as noted in the literature, can range from anywhere between pH 2 to pH 9.8 (Gräfe et al., 2009)), this results in the bauxite residue being able to cater for a wide range of pH (Gräfe et al., 2009) and also having the capability of removing both cations and anions from solution.

The SSA analysis carried out on the bauxite residues show an increase in specific surface area in all samples following treatment with either the gypsum or the seawater (Table 4). There was also an increase in pore volume following the addition of either gypsum or seawater (Table 4). This is attributed to the formation of precipitates formed in the neutralisation process of both gypsum and seawater and the effect of the Ca acting as a flocculant with the finer particles present. This increase in surface area also contributes to the increase in P adsorption following treatments. Although particle size affects adsorption onto media, due to the availability of sites for P uptake, no significant correlation was observed in the current study.

3.3. Implications of the findings of this study

The use of gypsum and seawater treatments on bauxite residue improved the overall P adsorption capacity of the bauxite residue samples, but mixing the bauxite residue and treatments with actual wastewater will be necessary to fully understand the total adsorption behaviour of the bauxite residue. In addition to improving the P adsorption, alkalinity was significantly reduced following both treatments; however, the EC was increased. This may limit the growth of plants on the gypsum or seawater-treated bauxite residues; therefore, one option may be to increase the rinsing period of the bauxite residue following treatment to remove the excess Ca^{2+} and Na^{+} ions in solution. Lowering the alkalinity, increasing the P, Ca^{2+} and Mg^{2+} content and improving the physical structure, provide the possible re-use option of using the treated bauxite residue as a growth media.

For a refinery, the cost of neutralisation techniques is an obvious consideration when deciding which technique(s) to use. The use of seawater as a neutralisation technique would be a cheap and feasible option for a refinery that is close to the sea. The establishment of a pipeline (if not already in place) would be the dominant capital cost. The use of a Nano filtration system to concentrate the Ca^{2+}, Mg^{2+} and Na^{+} ions in the seawater (Couperthwaite et al., 2014) could allow for the reduction in volume of seawater necessary for the neutralisation process, but may add to the cost. Gypsum however may be a more expensive option, requiring machinery such as amphirolls for the mixing and spreading of the gypsum. However, depending on the refinery's location, waste gypsum from construction sites or fossil fuel powered power stations may be used (Jones and Haynes, 2011).

4. Conclusions

This study examined the impact of gypsum and seawater treatments on the mineral, elemental and physiochemical properties of bauxite residue. The untreated bauxite residues were high in Fe and Al oxides and their mineralogical composition was dominated by Fe_2O_3, Al_2O_3, SiO_2 and CaO. Following treatment with gypsum and seawater, the pH decreased and EC increased, but no change was observed in the particle size or density. The SSA and pore volume of the bauxite increased following both treatments, which contributed to increased P adsorbency. Although the P adsorbency measured in this study was not as high as measured in other studies using different media, it still indicates that reuse in water or wastewater treatment facilities may be an appropriate option for bauxite residue.

Acknowledgements

The authors would like to acknowledge the financial support from the Irish Environmental Protection Agency (EPA) (2014-RE-MS-1) and the UK Natural Environment Research Council (NE/L01405X/1). The authors would also like to thank Rusal Aughinish Alumina and Alteo Gardanne, who provided the bauxite residue sand and mud samples.

Appendix A. Supplementary data

Supplementary data related to this article can be found at https://doi.org/10.1016/j.jclepro.2018.01.092.

References

Akhurst, D.J., Jones, G.B., Clark, M., McConchie, D., 2006. Phosphate removal from aqueous solutions using neutralised bauxite refinery residues (Bauxsol™). Environ. Chem. 3, 65–74.

Blake, G.R., 1965. Bulk density. In: Black, C.A. (Ed.), Methods of Soil Analysis. Part 1. Physical and Mineralogical Properties, Including Statistics of Measurement and Sampling. ASA, SSSA, Madison, WI, pp. 374–390.

Blake, G.R., Hartge, K.H., 1986. Particle density. In: Klute, A. (Ed.), Methods of Soil Analysis: Part 1—Physical and Mineralogical Methods. SSSA, ASA, Madison, WI, pp. 377–382.

12457–2 British Standard Institution, 2002. Characterisation of Waste. Leaching. Compliance Test for Leaching of Granular Waste Materials and Sludges. One Stage Batch Test at a Liquid to Solid Ratio of 10 L/kg for Materials with Particle Size below 4 mm (without or with Size Reduction).

Chen, N., Feng, C., Zhang, Z., Liu, R., Gao, Y., Li, M., Sugiura, N., 2012. Preparation and characterization of lanthanum (III) loaded granular ceramic for phosphorus adsorption from aqueous solution. J. Taiwan Inst. Chem. Eng. 43, 783–789.

Cooling, D.J., 2007. Improving the sustainability of residue management practices-Alcoa World Alumina Australia. In: Fouri, A., Jewell, R.J. (Eds.), Paste and Thickened Tailings: a Guide, vol. 316. http://citeseerx.ist.psu.edu/viewdoc/download?doi=10.1.1.629.1067&rep=rep1&type=pdf (accessed 31.10.17).

Couperthwaite, S.J., Johnstone, D.W., Mullett, M.E., Taylor, K.J., Millar, G.J., 2014. Minimization of bauxite residue neutralization products using nanofiltered seawater. Ind. Eng. Chem. Res. 53, 3787–3794.

Courtney, R.G., Timpson, J.P., 2005. Reclamation of fine fraction bauxite processing residue (red mud) amended with coarse fraction residue and gypsum. Water Air Soil Pollut. 164 (1–4), 91–102.

Courtney, R.G., Jordan, S.N., Harrington, T., 2009. Physico-chemical changes in bauxite residue following application of spent mushroom compost and gypsum. Land Degrad. Dev. 20, 572–581.

Courtney, R., Harrington, T., 2010. Assessment of plant-available phosphorus in a fine textured sodic substrate. Ecol. Eng. 36, 542–547.

Courtney, R., Kirwan, L., 2012. Gypsum amendment of alkaline bauxite residue–plant available aluminium and implications for grassland restoration. Ecol. Eng. 42, 279–282.

Danielson, R.E., Sutherland, P.L., 1986. Porosity. In: Klute, A. (Ed.), Methods of Soil Analysis. Part 1. Physical and Mineralogical Methods. SSSA, ASA, Madison, WI, pp. 443–461.

de Lima, A.C.A., Nascimento, R.F., de Sousa, F.F., Josue Filho, M., Oliveira, A.C., 2012. Modified coconut shell fibers: a green and economical sorbent for the removal of anions from aqueous solutions. Chem. Eng. J. 185, 274–284.

Dilmore, R.M., Howard, B.H., Soong, Y., Griffith, C., Hedges, S.W., DeGalbo, A.D., Morreale, B., Baltrus, J.P., Allen, D.E., Fu, J.K., 2009. Sequestration of CO2 in mixtures of caustic byproduct and saline waste water. Environ. Eng. Sci. 26, 1325–1333.

Eastham, J., Morald, T., Aylmore, P., 2006. Effective nutrient sources for plant growth on bauxite residue. Water Air Soil Pollut. 176 (1–4), 5–19.

Egemose, S., Sønderup, M.J., Beinthin, M.V., Reitzel, K., Hoffmann, C.C., Flindt, M.R., 2012. Crushed concrete as a phosphate binding material: a potential new management tool. J. Environ. Qual. 41, 647–653.

EPA, 1996. EPA Method 3050B: Acid Digestion of Sediments, Sludges, and Soils. www.epa.gov/sites/production/files/2015-06/documents/epa-3050b.pdf (accessed 30.10.2, 17).

EPA, 2014. Drinking Water Parameters Microbiological, Chemical and Indicator Parameters in the 2014 Drinking Water Regulations. www.epa.ie/pubs/advice/drinkingwater/2015_04_21_ParametersStandaloneDoc.pdf (accessed 30.10.2017).

European Commission, 2015. COM 2015. 614 Communication from the Commission to the European Parliament, the Council, the European Economic and Social Committee and the Committee of the Regions - Closing the Loop - an EU Action Plan for the Circular Economy. Brussels.
Evans, K., 2016. The history, challenges, and new developments in the management and use of bauxite residue. J. Sustain. Metall. 2, 316–331.
Fergusson, L., 2009. Commercialisation of Environmental Technologies Derived from Alumina Refinery Residues: a Ten-year Case History of Virotec. http://citeseerx.ist.psu.edu/viewdoc/download?doi=10.1.1.458.2073&rep=rep1&type=pdf (accessed 8.12.17).
Fois, E., Lallai, A., Mura, G., 2007. Sulfur dioxide absorption in a bubbling reactor with suspensions of Bayer red mud. Ind. Eng. Chem. Res. 46, 6770–6776.
Grace, M.A., Healy, M.G., Clifford, E., 2015. Use of industrial by-products and natural media to adsorb nutrients, metals and organic carbon from drinking water. Sci. Total Environ. 518, 491–497.
Grace, M.A., Clifford, E., Healy, M.G., 2016. The potential for the use of waste products from a variety of sectors in water treatment processes. J. Clean. Prod. 137, 788–802.
Goloran, J.B., Chen, C.R., Phillips, I.R., Xu, Z.H., Condron, L.M., 2013. Selecting a nitrogen availability index for understanding plant nutrient dynamics in rehabilitated bauxite-processing residue sand. Ecol. Eng. 58, 228–237.
Gräfe, M., Power, G., Klauber, C., 2009. Review of Bauxite Residue Alkalinity and Associated Chemistry. CSIRO, Australia. http://enfo.agt.bme.hu/drupal/sites/default/files/vörösiszpa%20kémia%20és%20lúgosság.pdf (accessed 12.12.17).
Hanahan, C., McConchie, D., Pohl, H., Creelman, R., Clark, M., Stocksiek, C., 2004. Chemistry of seawater neutralization of bauxite refinery residues (red mud). Environ. Eng. Sci. 21, 125–138.
Huang, W., Wang, S., Zhu, Z., Li, L., Yao, X., Rudolph, V., Haghseresht, F., 2008. Phosphate removal from wastewater using red mud. J. Hazard. Mater. 158, 35–42.
IAI, 2015. Bauxite residue Management: Best Practice. http://www.world-aluminium.org/media/filer_public/2015/10/15/bauxite_residue_management_-_best_practice_english_oct15edit.pdf (accessed 14.10.2017).
Jacukowicz-Sobala, I., Ociński, D., Kocioł ek-Balawejder, E., 2015. Iron and aluminium oxides containing industrial wastes as adsorbents of heavy metals: application possibilities and limitations. Waste Manag. Res. 33, 612–629.
Johnston, M., Clark, M.W., McMahon, P., Ward, N., 2010. Alkalinity conversion of bauxite refinery residues by neutralization. J. Hazard. Mater. 182, 710–715.
Jones, B.E., Haynes, R.J., 2011. Bauxite processing residue: a critical review of its formation, properties, storage, and revegetation. Crit. Rev. Environ. Sci. Technol. 41, 271–315.
Jones, B.E., Haynes, R.J., Phillips, I.R., 2012. Addition of an organic amendment and/or residue mud to bauxite residue sand in order to improve its properties as a growth medium. J. Environ. Manag. 95, 29–38.
Kirwan, L.J., Hartshorn, A., McMonagle, J.B., Fleming, L., Funnell, D., 2013. Chemistry of bauxite residue neutralisation and aspects to implementation. Int. J. Miner. Process. 119, 40–50.
Klauber, C., Gräfe, M., Power, G., 2011. Bauxite residue issues: II. options for residue utilization. Hydrometallurgy 108, 11–32.
Lehoux, A.P., Lockwood, C.L., Mayes, W.M., Stewart, D.I., Mortimer, R.J., Gruiz, K., Burke, I.T., 2013. Gypsum addition to soils contaminated by red mud: implications for aluminium, arsenic, molybdenum and vanadium solubility. Environ. Geochem. Health 35, 643–656.
Li, L.Y., 2001. A study of iron mineral transformation to reduce red mud tailings. Waste Manag. 21, 525–534.
Li, Y., Liu, C., Luan, Z., Peng, X., Zhu, C., Chen, Z., Zhang, Z., Fan, J., Jia, Z., 2006. Phosphate removal from aqueous solutions using raw and activated red mud and fly ash. J. Hazard. Mater. 137, 374–383.
Liu, Y., Lin, C., Wu, Y., 2007. Characterization of red mud derived from a combined Bayer Process and bauxite calcination method. J. Hazard. Mater. 146, 255–261.
Liu, W., Chen, X., Li, W., Yu, Y., Yan, K., 2014. Environmental assessment, management and utilization of red mud in China. J. Clean. Prod. 84, 606–610.
Lopez, E., Soto, B., Arias, M., Nunez, A., Rubinos, D., Barral, M.T., 1998. Adsorbent properties of red mud and its use for wastewater treatment. Water Res. 32, 1314–1322.
Mayes, W.M., Burke, I.T., Gomes, H.I., Anton, A.D., Molnár, M., Feigl, V., Ujaczki, É., 2016. Advances in understanding environmental risks of red mud after the Ajka spill, Hungary. J. Sustain. Metall. 2, 332–343.
Menzies, N.W., Fulton, I.M., Morrell, W.J., 2004. Seawater neutralization of alkaline bauxite residue and implications for revegetation. J. Environ. Qual. 33, 1877–1884.
McBride, M.B., 2000. Chemisorption and Precipitation Reactions. Handbook of Soil Science. CRC Press, Boca Raton, FL, pp. B265–B302.
McConchie, D., Clark, M., Davies-McConchie, F., 2001. Processes and Compositions for Water Treatment. Neauveau Technology Investments, Australian, p. 28.
Newson, T., Dyer, T., Adam, C., Sharp, S., 2006. Effect of structure on the geotechnical properties of bauxite residue. J. Geotech. Geoenviron. 132, 143–151.
Palmer, S.J., Frost, R.L., 2009. Characterisation of bauxite and seawater neutralised bauxite residue using XRD and vibrational spectroscopic techniques. J. Mater. Sci. 44, 55–63.
Power, G., Gräfe, M., Klauber, C., 2011. Bauxite residue issues: I. Current management, disposal and storage practices. Hydrometallurgy 108, 33–45.
Pradhan, J., Das, S.N., Das, J., Rao, S.B., Thakur, R.S., 1996. Characterization of Indian red muds and recovery of their metal values. In: Annual Meeting and Exhibition of the Minerals, Metals and Materials Society, Anaheim, CA, 4 – 8 February 1996.
Prajapati, S.S., Najar, P.A., Tangde, V.M., 2016. Removal of phosphate using red mud: an environmentally hazardous waste by-product of alumina industry. Adv. Phys. Chem. 2016.
Snars, K., Gilkes, R.J., 2009. Evaluation of bauxite residues (red muds) of different origins for environmental applications. Appl. Clay Sci. 46, 13–20.
Thomas, G.W., 1982. Exchangeable Cations. Methods of Soil Analysis. Part 2. Chemical and Microbiological Properties, (Methodsofsoilan2), pp. 159–165.
Vakros, J., Kordulis, C., Lycourghiotis, A., 2002. Potentiometric mass titrations: a quick scan for determining the point of zero charge. Chem. Commun. 17, 1980–1981.
Vohla, C., Alas, R., Nurk, K., Baatz, S., Mander, Ü., 2007. Dynamics of phosphorus, nitrogen and carbon removal in a horizontal subsurface flow constructed wetland. Sci. Total Environ. 380, 66–74.
Wang, S., Ang, H.M., Tadé, M.O., 2008. Novel applications of red mud as coagulant, adsorbent and catalyst for environmentally benign processes. Chemosphere 72, 1621–1635.
Wang, B., Lehmann, J., Hanley, K., Hestrin, R., Enders, A., 2015. Adsorption and desorption of ammonium by maple wood biochar as a function of oxidation and pH. Chemosphere 138, 120–126.
Wang, Z., Shen, D., Shen, F., Li, T., 2016. Phosphate adsorption on lanthanum loaded biochar. Chemosphere 150, 1–7.
Xue, S., Zhu, F., Kong, X., Wu, C., Huang, L., Huang, N., Hartley, W., 2016. A review of the characterization and revegetation of bauxite residues (Red mud). Environ. Sci. Pollut. Res. 23, 1120–1132.
Ye, J., Zhang, P., Hoffmann, E., Zeng, G., Tang, Y., Dresely, J., Liu, Y., 2014. Comparison of response surface methodology and artificial neural network in optimization and prediction of acid activation of Bauxsol for phosphorus adsorption. Water Air Soil Pollut. 225 (12), 2225.
Zhu, F., Li, Y., Xue, S., Hartley, W., Wu, H., 2016. Effects of iron-aluminium oxides and organic carbon on aggregate stability of bauxite residues. Environ. Sci. Pollut. Res. 23, 9073–9081.